Journal of Hazardous Materials xxx (xxxx) xxxx

Contents lists available at ScienceDirect

Journal of Hazardous Materials

journal homepage: www.elsevier.com/locate/jhazmat

Mechanism of microbial dissolution and oxidation of antimony in stibnite under ambient conditions

Prakash C. Loni[a,b,1], Mengxiaojun Wu[a,b,1], Weiqi Wang[a,b], Hongmei Wang[a,b,*], Liyuan Ma[b], Chaoyang Liu[a], Yuyang Song[a], Olli H Tuovinen[c]

[a] State Key Laboratory of Biogeology and Environmental Geology, China University of Geosciences, Wuhan, 430074, China
[b] School of Environmental Studies, China University of Geosciences, Wuhan, 430074, China
[c] Department of Microbiology, Ohio State University, Columbus, OH 43210, USA

GRAPHICAL ABSTRACT

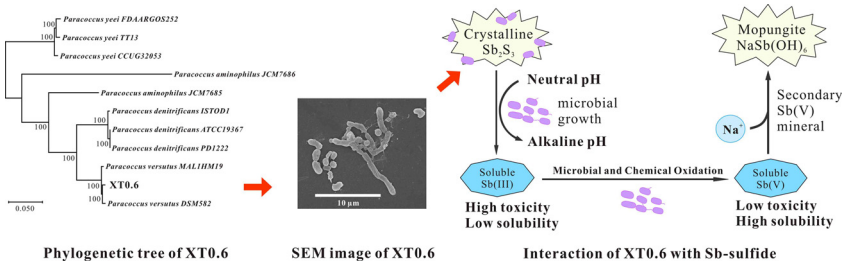

ARTICLE INFO

Editor: Rinklebe Jörg

Keywords:
Xikuangshan
Paraccocus versutus XT0.6
Antimony sulfide bearing ores
Antimony dissolution and oxidation

ABSTRACT

In this study, we demonstrate that a bacterial isolate *Paraccocus versutus* XT0.6 from the Xikuangshan antimony mine, the world largest antimony deposit, is capable of stibnite dissolution, oxidation of Sb(III), and formation of secondary Sb(V) bearing mineral. The isolate could oxidize dissolved Sb(III) aerobically and anaerobically. It was able to dissolve Sb(III) in solid minerals, which was subsequently oxidized to Sb(V) completely. Part of Sb(V) was scavenged by the formation of secondary Sb(V)-bearing mineral mopungite [$NaSb(OH)_6$] in the biotic experiments. In contrast, Sb(III) released from mineral/rocks was only partially oxidized to Sb(V) and no secondary Sb-bearing mineral was formed in abiotic controls. These results demonstrated that microbial processes involved in the mobilization, oxidation, and transformation of antimony in minerals/rocks under ambient environmental conditions and offer new insights in biogeochemistry of Sb at mining areas.

1. Introduction

Human activities such as mining and utilization of antimony in various industries (He et al., 2018; Li et al., 2016a; Wilson et al., 2010) result in the contamination of antimony in soil, sediments and aquatic environments, posing great risk to ecosystems. For example, the concentrations of antimony have reached 1160 mg/kg, 0.5–2.0 mg/kg and 29 mg/L, respectively, in soils, sediments and water bodies around major mining regions of China (He et al., 2012). These levels are many orders of magnitude higher than the set threshold concentration in drinking water proposed by World Health Organization (20 μg/L) and the Ministry of Health, China (MOHC) (5 μg/L) (WHO, 1996; He, 2007a). As one of the priority pollutants (He et al., 2012; Filella et al., 2002), the toxicity and mobility of Sb are greatly influenced by its

* Corresponding author at: State Key Laboratory of Biogeology and Environmental Geology, China University of Geosciences, Wuhan, 430074, China.
E-mail addresses: hmwang@cug.edu.cn, wanghmei04@163.com (H. Wang).
[1] Equal contribution to this manuscript.

https://doi.org/10.1016/j.jhazmat.2019.121561
Received 27 July 2019; Received in revised form 15 September 2019; Accepted 27 October 2019
0304-3894/

chemical and redox speciation. Sb(III) and Sb(V) are two forms commonly found in natural environments (Wilson et al., 2010; Filella et al., 2003; Jinming et al., 2015) and Sb(III) is more toxic (Wang et al., 2011; Cornelis et al., 2005) and less motile than Sb(V) (Leuz et al., 2006; Buschmann and Sigg, 2004). It is thus of great significance to understand the oxidation and transformation of Sb in natural environments as these reactions will greatly enhance our understanding about Sb geochemical circulations and their environmental impacts.

An important geochemical process of antimony in nature is the dissolution and oxidation of Sb(III) from Sb-bearing minerals and rocks. Antimony dissolution from minerals is a pH-dependent process (Biver and Shotyk, 2012a; Hu et al., 2015a; Khan et al., 2019). For example, Sb-sulfide minerals dissolve under alkaline conditions (Hu et al., 2015a, a) and Sb-oxide minerals require acidic conditions for the dissolution (Multani et al., 2016; Li et al., 2016b). Abiotic factors such as light (sunlight, ultraviolet light, simulated sunlight) irradiation (Hu et al., 2015b, 2014) dissolved O_2, some cations (Ca^{2+},Mg^{2+}) (Biver and Shotyk, 2012a) and low molecular weight dissolved organic matter (Biver and Shotyk, 2012b; Hu and He, 2017) may play a part in the dissolution of Sb-minerals. Although microbial release and biotransformation of arsenic (similar chemical properties with antimony)-bearing minerals was already reported (Paul et al., 2015; Zhang et al., 2017, 2016), and the enhancing role of microorganisms in the release of Sb from minerals has been established in acid bioleaching studies (Nguyen et al., 2015), but the underlying factors are largely unexplored and not elucidated for ambient, circumneutral pH conditions.

Sb(III) dissolved from minerals can be subsequently oxidized either by abiotic or biotic processes, altering the toxicity and mobility of antimony in aquatic environments (Li et al., 2016b; Hu et al., 2014; Terry et al., 2015; Abin and Hollibaugh, 2014; Kulp et al., 2015; Hu et al., 2017). The abiotic oxidation of Sb(III) is very slow at neutral and alkaline (pH 8.5) conditions with a half-life of 170 years (Leuz and Johnson, 2005; Asta et al., 2012), suggesting that it is the biotic oxidation that contributes to high Sb(V) concentrations found in alkaline environments (Herath et al., 2017). Several studies have shown that various bacteria are capable of oxidation of dissolved Sb(III) at rates of < 0.1 to 333 μM/d (Lu et al., 2018; Lehr et al., 2007; Li et al., 2013; Shi et al., 2013; Nguyen et al., 2017; Li et al., 2018; Nguyen and Lee, 2015). Most of these bacterial isolates belong to *Proteobacteria* (Wang et al., 2016), and the dominance of the phylum *Proteobacteria* was observed throughout Sb-contaminated sediments, watersheds and soils (Wang et al., 2016; Xiao et al., 2016; Sun et al., 2016). A cellular mechanism of the microbial oxidation of dissolved Sb(III) has been proposed, which includes intracellular enzymatic catalysis and oxidation by cellular H_2O_2 (Li et al., 2015, 2017).

Although the microbial role and molecular mechanism in the oxidation of dissolved Sb(III) have been investigated under laboratory conditions (Li et al., 2015), processes involved in the oxidation of Sb (III) trapped in minerals and pristine rocks at mining areas remain poorly understood. We hypothesize that bacteria can dissolve Sb-bearing minerals via changing pH and subsequently oxidize the dissolved Sb(III) to Sb(V), and thus play an important role in the biogeochemistry of antimony. To test the hypothesis, we isolated a bacterium from mine tailing samples at the Xikuangshan antimony mine in Central China and investigated its role in the release and redox speciation of antimony from Sb-sulfide samples. To our knowledge, this is the first report to demonstrate bacterially-mediated dissolution and oxidation of antimony associated with pristine Sb-bearing rocks.

2. Materials and methods

2.1. Sampling site

The Xikuangshan (XKS) antimony mine, the world's largest antimony mine, located in the Lengshuijiang city, in the middle of Hunan Province, Central China. The XKS deposit is about 2 km wide and 9 km long and the ore reserves contain stibnite (Sb_2S_3) as the main ore mineral and quartz, calcite, and pyrite as the gangue minerals (He, 2007b). Smelter residues with high levels of antimony and other metals (As, Al, Mn, Fe) have been disposed in the tailings dam over the years (Liu et al., 2010). Groundwater at the site is neutral to slightly alkaline (7.9–8.5) (Wen et al., 2016) and the concentration of total dissolved Sb reached up to 29.4 mg/L (241 μM) (Wen et al., 2016). Mine tailing samples (aprrox. 50 g each) were collected for bacterial isolation with a tube soil drill at the depth of 0.2 to 1.6 m with an interval of 0.2 m between each sample and stored in sterile bags at 4 °C. Rock samples from mining tunnels 5, 25 and 27 (designated as 5 M, 25 M and 27 M, respectively) were collected to investigate the microbial dissolution and oxidation of Sb(III) in Sb-bearing rocks with a sterilized shovel and stored in sterile bags at 4 °C. All samples were shipped refrigerated to the laboratory within one week for further analysis.

2.2. Isolation and identification of antimony oxidizing bacteria

One gram of mine tailing residues was inoculated into 100 mL of sterile modified chemically defined media (CDM) (Weeger et al., 1999) amended with 50 μM Sb(III) added as antimony potassium tartrate ($C_8H_4K_2O_{12}Sb_2{\cdot}0.5H_2O$, from Sigma-Aldrich) and incubated at 30 °C with 150 rpm. The initial pH was set at 7.2 (Weeger et al., 1999). After 5 days of incubation, the enrichment culture was serially diluted up to 10^{-4} in sterile saline and streaked onto CDM agar plates amended with 50 μM Sb(III). Colonies were subsequently purified by re-streaking several times on antimony amended CDM plates. Colonies were transferred to liquid media and screened qualitatively for dissolved Sb(III) oxidation using the $KMnO_4$ method (Salmassi et al., 2002). Isolates were stored in glycerol (20 %) medium at −80 °C.

Whole genome sequencing of XT0.6 was conducted at Personalbio (Shanghai, China) and assembled with Illumina Miseq reads and Pacbio reads (Lu et al., 2018). OrthoMCL (http://orthomcl.org/orthomcl/) was used to analyze Ortholog Cluster Groups. Common orthologous single-copy genes were used to construct the phylogenetic tree through FastTree (http://www.microbesonline.org/fasttree/).

2.3. Setup of experiments

2.3.1. Microbial oxidation of dissolved Sb(III) under aerobic and anaerobic conditions

Aerobic Sb(III) oxidation experiments were performed in 250 mL conical flasks containing 100 mL sterile CDM with 100–400 μM of Sb (III) at 30 °C with 150 rpm in the dark. The media were inoculated with XT0.6 previously grown in CDM without any Sb. Samples were collected every 12 h and the supernatants were stored at 4 °C for dissolved Sb speciation analysis. Abiotic controls without bacterial inoculum were run under parallel conditions. Each experimental set was run in duplicates.

For anaerobic oxidation experiments, serum bottles with CDM, stock solutions of Sb(III), and nitrate were purged separately with N_2 for 20 min and another 15 min in the headspace. The serum bottles with CDM were capped with septa and aluminum crimps, and subsequently sterilized at 120 °C for 20 min. The stock solutions of nitrate and Sb(III) were filter sterilized and added into the serum bottles with CDM with a final concentration of 1.5 mM (nitrate in each bottle) and 100, 150, and 200 μM (Sb(III) respectively using sterile syringes. The media were inoculated (1 % v/v) with XT0.6 in exponential phase in CDM without any Sb and incubated at 30 °C under static conditions. Samples were collected daily. Abiotic controls were run in tandem with biotic cultures in each experimental set. All experiments were conducted in duplicate in an anaerobic glove box (Vacuum Airlock AC17-022, Coy Laboratory Products, Grass Lake, MI).

2.3.2. Measurement of the kinetics of dissolved Sb(III) oxidation

Kinetic study of dissolved Sb(III) oxidation was carried out under

aerobic condition. Overnight culture grown in CDM without Sb was harvested by centrifugation at 1681 *g* for 20 min at 4 °C. Cells were washed twice with tris − HCl buffer (10 mM) at pH 7.2. Washed cells were re-suspended into tris − HCl buffer to reach the density of about 1.2×10^7 cells/ml which was counted by hemocytometer. Oxidation started with the addition of Sb(III) with a final concentration of 10 μM to 400 μM into cell suspension buffer. Control was set in the buffer without cells. Samples were collected with an interval 20 min and cells were removed by centrifugation followed by filtration. The supernatant was stored at − 20 °C until antimony speciation analysis. Kinetic rates were calculated following the Michaelis-Menten Eq. (1) and the values of V_{max} and K_m were obtained by Lineweaver-Burk plot (Das et al., 2016).

$$v = \frac{Vmax[S]}{Km + [S]} \quad (1)$$

Here, v (μM/min) denotes reaction rate of microbial oxidation and [S] represents substrate concentration. Whereas V_{max} (μM/min) is the maximum velocity of Sb(III) oxidation and K_m is the Michaelis-Menten equation constant.

2.3.3. Bacterial dissolution and oxidation of Sb(III) in stibnite and rock samples

To understand the impact of Sb-bearing mineral content on Sb dissolution, commercial Sb_2S_3 (97.19 %, Stibnite) (purchased from Aladdin Industrial Corp., Shanghai) and three Sb-bearing rock samples from the XKS mining area were selected in the study. The samples were ground to 200 mesh for the experiments. Samples (0.1 g) were added to 100 mL CDM and sterilized for 20 min at 120 °C. After cooling, bacteria was inoculated (1 % v/v) from CDM culture grown without Sb(III). The media for the abiotic experiments were adjusted to initial pH 7.2, 8.2 and 9.3 respectively. The cultures and un-inoculated abiotic controls were incubated at 30 °C at 150 rpm in the dark. Samples were collected daily. Biomass was separated by centrifugation at 9400*g* for 10 min, and the supernatants were filter sterilized and stored at 4 °C for dissolved antimony speciation analysis. All experimental sets were run in duplicate under aerobic conditions.

2.4. Analytical methods

Bacterial cell density was measured with a UV–vis spectrophotometer at 600 nm after 20 min quiet sitting to avoid the impact of mineral particles. The pH values were measured using a multi-parameter water quality analyzer (Hach Co., Loveland, CO). Total alkalinity was determined by titration with 0.2 M HCl (Kaksonen et al., 2003). Speciation of dissolved antinomy in supernatant samples was conducted by HPLC (LC-20AT, Shimadzu, Tokyo) and quantified by hydride generation atomic fluorescence spectroscopy (SA-10, Beijing Titan Instruments Co.).

Solid residues from cultures were collected by centrifugation at 2600*g* for 10 min, treated with 10 % SDS to remove organic matter and freeze dried (Alpha 1–2/LD Christ, Germany) at − 55 °C with 0.10 mbar pressure for overnight. Solids in abiotic controls were collected and freeze dried directly. Mineral phases of all biotic experiments and abiotic controls were analyzed using X-ray diffraction (XRD, Bruker AXS D8- Focus) equipped with Cu-Kα radiation at 40 kV and 40 mA. Samples were scanned from 5 to 90° 2θ at 2° 2θ/min. Quantification of XRD patterns was done by X ray Run 2.0 based on the least square method (with PDF 74–1046 for Sb_2S_3, PDF 75-0443 for quartz, PDF 83-0578 for calcite, and PDF 85-0363 for mopungite) (Kong et al., 2019; Zhou et al., 2019). Morphology of minerals and bacterial cells was observed with SEM (acceleration voltage 30.0 kV, probe current 10.0 μA) used high vacuum and secondary electron imaging equipped with EDS (Hitachi SU8010). Prior to SEM imaging, the samples on glass slides were dehydrated with an ethanol series and fixed with critical point drying (Quorum K850, Nanjing Tansi Technology) (Liu et al., 2012).

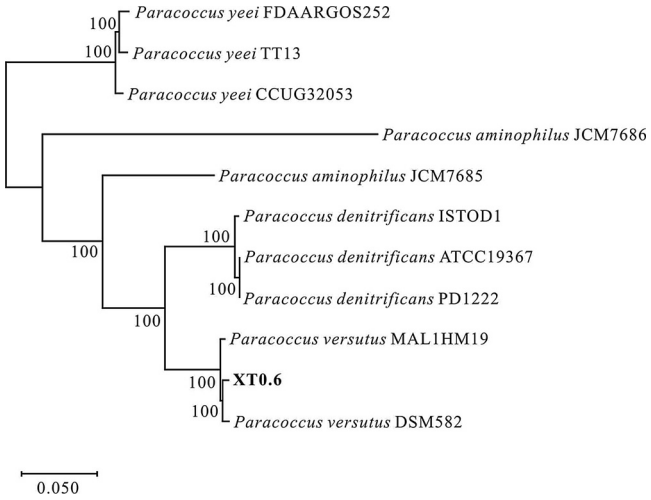

Fig. 1. The phylogenetic tree of XT0.6 was constructed by the maximum likelihood method (bootstrap = 1000, LG + I+G + F model) using 1749 single-copy orthologous genes.

3. Results and discussion

3.1. Microbial oxidation of dissolved Sb(III)

The isolate XT0.6 was identified as *Paracoccus versutus* (Fig. 1). The cells were elongated and formed chains (Fig. S1A) with rough surfaces (Fig. S1B) when Sb(III) was present, but were short rods (Fig. S1C) with smooth surfaces when Sb(III) was absent (Fig. S1D). The morphological change of XT0.6 in the presence of Sb(III) may indicate cell response to metalloid stress which leads to the elongation (Nepple et al., 1999). Isolate XT0.6 oxidized dissolved Sb(III) under both aerobic and anaerobic conditions (Fig. 2). Within 24 h 300 μM Sb(III) was completely oxidized by XT0.6 under aerobic conditions. No growth or oxidation was observed at 400 μM Sb(III) even after extended incubation. In the aerobic oxidation of dissolved Sb(III), Sb(III) decrease was coupled with a corresponding increase in the concentration of Sb(V) (Fig. 2A). The pH of culture medium increased from 7.2 to 9.2 after 48 h and alkalinity increased to 1160 mg/L during the incubation (Fig. S2). The isolate could also completely oxidize 100 μM Sb(III) within 24 h under anaerobic conditions (Fig. 2B). Increasing concentrations of initial dissolved Sb(III) to150 μM and 200 μM slowed down the bacterial growth and more time (72 h and 96 h) was needed to completely oxidize the dissolved Sb(III) under anaerobic conditions (Fig. S3A, B). The Sb(III) concentrations in the abiotic controls under aerobic and anaerobic conditions were relatively unchanged throughout the incubation (Fig. 2).The oxidation of 10–400 μM dissolved Sb(III) by cell suspensions (1.2×10^7 cells/mL) yielded an apparent K_m (the Michaelis-Menten equation constant) of 148.1 μM (Fig. 3, Table S1). However, due to different incubation and calculation methods (unit) adopted by different authors, the direct comparison of kinetics parameters was difficult.

To date, several heterotrophic bacterial genera, mainly affiliated with *Proteobacteria*, have been reported to be able to oxidize dissolved Sb(III) under aerobic conditions (Lu et al., 2018; Lehr et al., 2007; Li et al., 2013; Shi et al., 2013; Nguyen et al., 2017; Li et al., 2018; Nguyen and Lee, 2015). Previously reported oxidation rates of dissolved Sb(III) vary from < 1 μM/d to 333.3 μM/d (Table S2), with 300 μM/d determined for XT0.6 in this study. The oxidation rates of dissolved Sb(III) under anaerobic conditions are in the range of 31.2–66.6 μM/d (Terry et al., 2015; Nguyen et al., 2017). Strain XT0.6 had the highest oxidation rate of 100 μM/d in comparison with two bacterial isolates

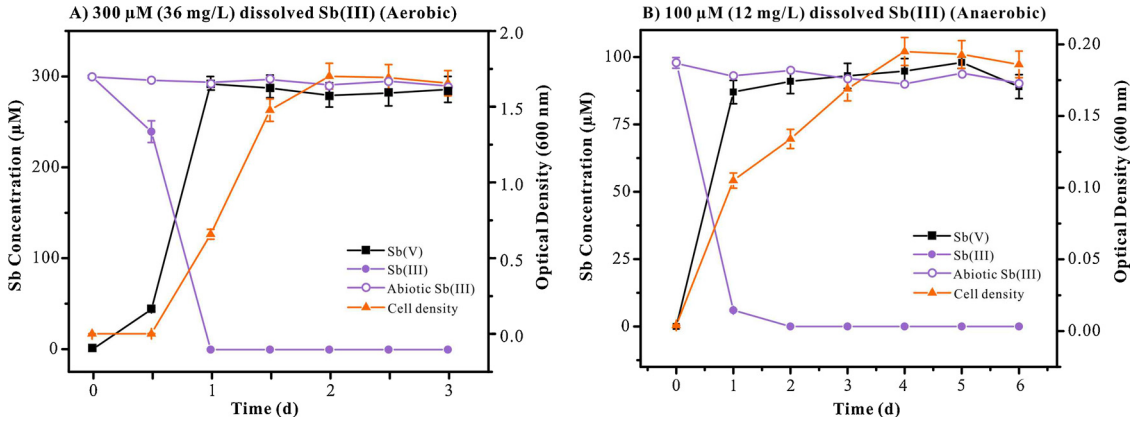

Fig. 2. Oxidation of dissolved Sb(III) by XT0.6 under aerobic (A) and anaerobic conditions (B–D). Error bars indicates the standard deviation (n = 2).

previously reported under anaerobic conditions, with lactate as the electron donor and nitrate as the electron acceptor.

3.2. Bacterial oxidation of Sb(III) in mineral phases

The dissolution and oxidation experiments were conducted under aerobic conditions with an initial pH of 7.2 at 30 °C to understand the changes of Sb speciation after the exposure of Sb-bearing minerals/rocks to atmosphere during mining activities. The commercial Sb_2S_3 and the ground rock samples of 25 M, 27 M and 5 M with various content of stibnite (Table 1) were used. In all bacterial treatments, the pH increased from 7.2 to 8.5 within one day and subsequently continued to rise to 9.3 (Fig. 4). The pH values in the abiotic controls initially decreased and stabilized at pH 6.3 at the end of the time course (Fig. 4). Under abiotic conditions, only Sb(III) was detected and its maximum concentration stayed at 33 mg/L (271 µM) for the standard stibnite sample and at 14 mg/L (115 µM), 16 mg/L (131 µM) and 15 mg/L (123 µM) for the rock samples of 27 M, 25 M and 5 M, respectively (Fig. 4). In contrast, 5-23 mg/L (41–189 µM) Sb(III) was initially present in bacterial cultures but was depleted within a day and was not detectable for the rest of the time course (Fig. 4). The concentration of dissolved Sb(V) increased within the first 4–5 days (Fig. 4), and reached the maximum concentration of 68 mg/L (559 µM) (Fig. 4A), 58 mg/L (476 µM) (Fig. 4B), 65 mg/L (534 µM) (Fig. 4C) and 86 mg/L (706 µM) (Fig. 4D) on days 4, 5, 8 and 9 with the addition of standard stibnite and the rock samples 27 M, 25 M and 5 M, respectively. Subsequently the concentration of Sb(V) decreased in all cultures, suggesting precipitation of Sb(V)-bearing secondary minerals. Optical density of cells reached the maximum at 60 h in all cultures (Fig. S4).

Table 1
The relative contents (wt%) of mineral phases of samples before and after 13 days of incubation at different pH.

Solid material used		Sb_2S_3 (%)	SiO_2 (%)	$Ca(CO)_3$ (%)	$NaSb(OH)_6$ (%)
Stb	Initial	97.19	2.81	–	–
	Abiotic (7.2)	82.20	17.80	–	–
	Abiotic (8.2)	89.75	10.07	–	–
	Abiotic (9.3)	81.87	18.08	–	–
	Biotic(7.2)	**74.45**	**17.30**	–	**8.25**
27M	Initial	40.83	59.17	–	–
	Abiotic (7.2)	30.50	69.50	–	–
	Abiotic (8.2)	18.78	81.22	–	–
	Abiotic (9.3)	21.64	78.38	–	–
	Biotic(7.2)	**21.01**	**68.99**	–	**10.00**
25M	Initial	56.93	19.38	23.69	–
	Abiotic (7.2)	40.54	26.76	32.70	–
	Abiotic (8.2)	24.84	41.07	34.07	–
	Abiotic (9.3)	8.66	40.48	50.85	–
	Biotic(7.2)	**28.89**	**30.05**	**31.24**	**9.82**
5M	Initial	29.78	70.22	–	–
	Abiotic (7.2)	23.28	76.71	–	–
	Abiotic (8.2)	14.83	85.19	–	–
	Abiotic (9.3)	16.22	83.78	–	–
	Biotic(7.2)	**16.49**	**73.31**	–	**10.20**

Note: Stb: stibnite; 27 M, 25 M and 5 M are the rock samples collected from mining tunnel 27, 25 and 5 at XKS, Hunan province, respectively. Numbers in the parenthesis are pH values.

3.3. Impact of alkaline pH on Sb(III) dissolution and oxidation in mineral phases

To distinguish the impact of pH on the dissolution and oxidation of Sb(III) in minerals, abiotic experiments were also conducted at initial

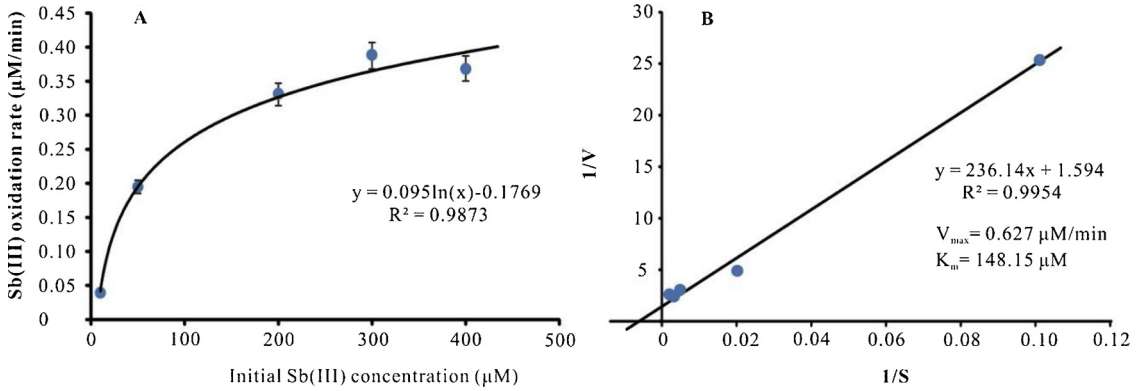

Fig. 3. Oxidation kinetics of dissolved Sb(III)mediated by XT0.6.A) Oxidation rate at different initial concentrations of dissolved Sb(III). B) Oxidation rate data fit to the Lineweaver-Burk plot to determine V_{max} and K_m values. Error bars in A) indicates the standard deviation (n = 2).

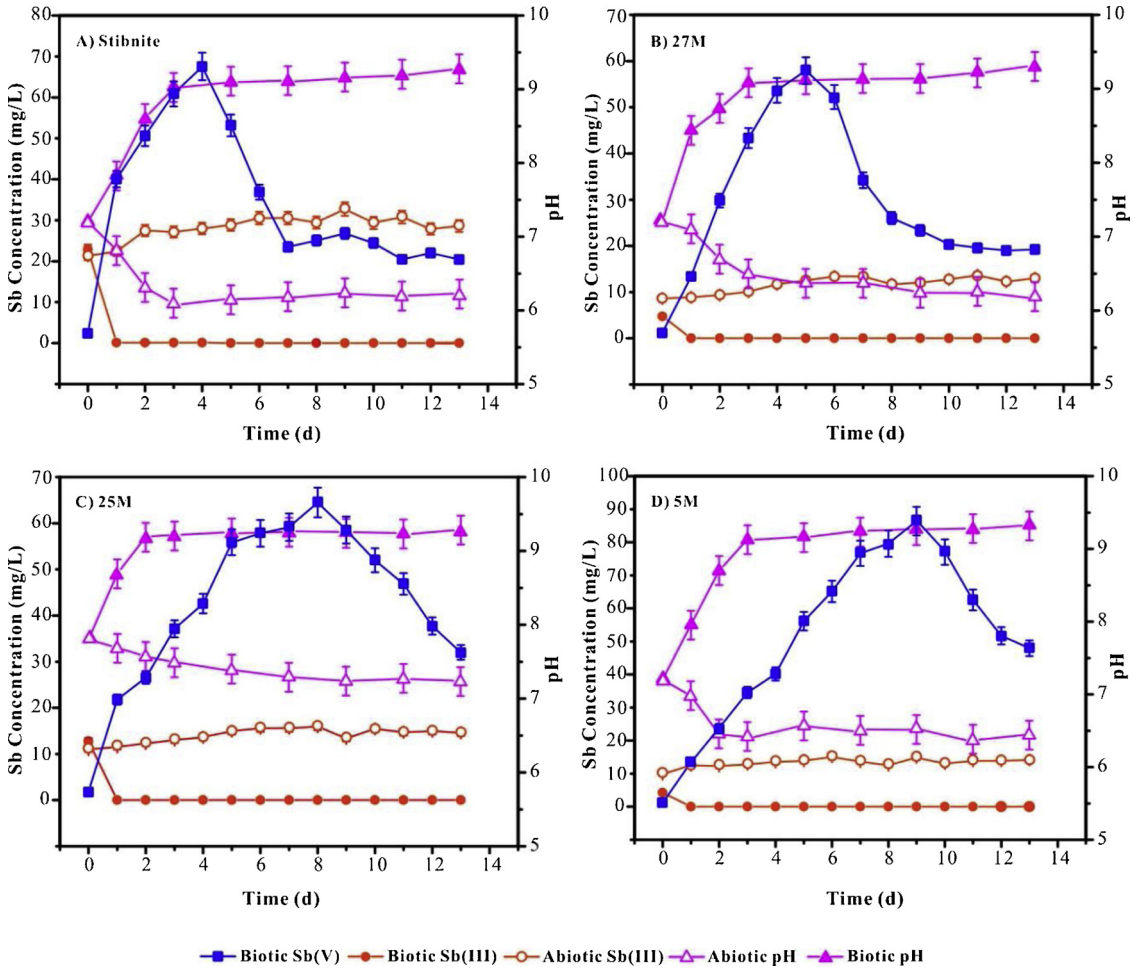

Fig. 4. Changes in pH and concentrations of dissolved Sb(III) and Sb(V) in XT0.6 cultures and their abiotic counterparts versus time with the addition of standard stibnite (A), ore rock samples from tunnel 27(B), 25(C) and 5(D). Error bars indicate the standard deviation (n = 2).

pH 8.2 and 9.3. Overall an increase in concentrations of the total dissolved Sb and Sb(V) was observed with the increase of the initial pH (Fig. 5, Table S3). At initial pH 8.2, the concentrations of Sb(III) were higher than or comparable to those of Sb(V) (Fig. 5). The maximum concentration of total dissolved Sb reached up to 61 mg/L [501 μM, 33.9 % Sb(V)] with the addition of 27 M rock sample (Table S3). At initial pH 9.3, the highest concentration of total dissolved Sb was 88 mg/L (723 μM), and 70 % of it was oxidized to Sb(V) in the system with the addition of stibnite (Fig. 5 and Table S3). Contrasting with the biotic experiments, the pH values decreased throughout the time course (Fig. 5), and Sb(III) and Sb(V) coexisted in these abiotic experiments.

The dissolution of antimony from the mineral phase and the redox state of antimony are significantly impacted by pH. For example, more antimony was dissolved from Sb-sulfide under alkaline conditions (pH 9.8) than under acidic condition (pH 2.0) (Hu et al., 2017, 2016b). This trend is also consistent with our abiotic results as the total Sb dissolved increased with the increase of pH (Table S3). The pH increased from 7.2 to 9.3 in the culture of strain XT0.6 during growth with lactate and thus favored the dissolution of Sb from the mineral phases. The highest concentration of dissolved Sb reached 86 mg/L (706 μM) after 13 days' incubation with XT0.6 in 5 M powder suspensions (Fig. 4D). The dissolved Sb was completely oxidized to Sb(V) in the XT0.6 cultures, whereas Sb(III) and Sb(V) coexisted in abiotic systems throughout the time course. This strongly confirmed the microbial role in the complete oxidation of Sb(III).

Conflicting with some previous reports (Leuz and Johnson, 2005; Asta et al., 2012) about the extremely slow abiotic dark oxidation of Sb (III) under alkaline aerobic conditions (pH 8.5), we observed an increase in Sb(III) oxidation with the increase of pH in the abiotic systems (Table S3). At initial pH 7.2, chemical oxidation of Sb(III) was not detected, but it distinctly increased at initial pH 8.2 and 9.3 (Table S3). Up to 70 % of dissolved Sb can be oxidized in the abiotic system with stibnite addition at pH 9.3. Therefore under alkaline conditions both the microbial and chemical oxidation of Sb(III) was confirmed in our experimental systems. Bacteria enhanced the dissolution of Sb by increasing the pH and subsequently contributed to the complete oxidation of dissolved Sb(III) to Sb(V). Given that the pH of the groundwater at the XKS has varied between 7.9–8.5, both microbial and chemical factors are involved in the dissolution and oxidation of Sb-bearing minerals, thus resulting in elevated concentrations of Sb(V) in the groundwater in the study area. However, their contributions may vary with pH values and microorganisms may play more important role under neutral conditions.

3.4. Transformation of mineral phases during Sb dissolution and oxidation

Stibnite and quartz were detected in all mineral/rock samples used in this study (Fig. 6). The 25 M rock sample also contained about 33 % calcite (Fig. 6, Table 1). The Sb_2S_3 contents of the stibnite and the rock samples 25 M, 27 M and 5 M were 97.19 %, 56.93 %, 40.83 % and 29.78 %, respectively (Table 1). After 13 days of incubation with strain XT0.6, the stibnite content of standard stibnite had decreased by about 23 %. The corresponding stibnite decrease in the rock samples 25 M, 27 M and 5 M were 28 %, 20 %, and 13 %, respectively. In contrast, the

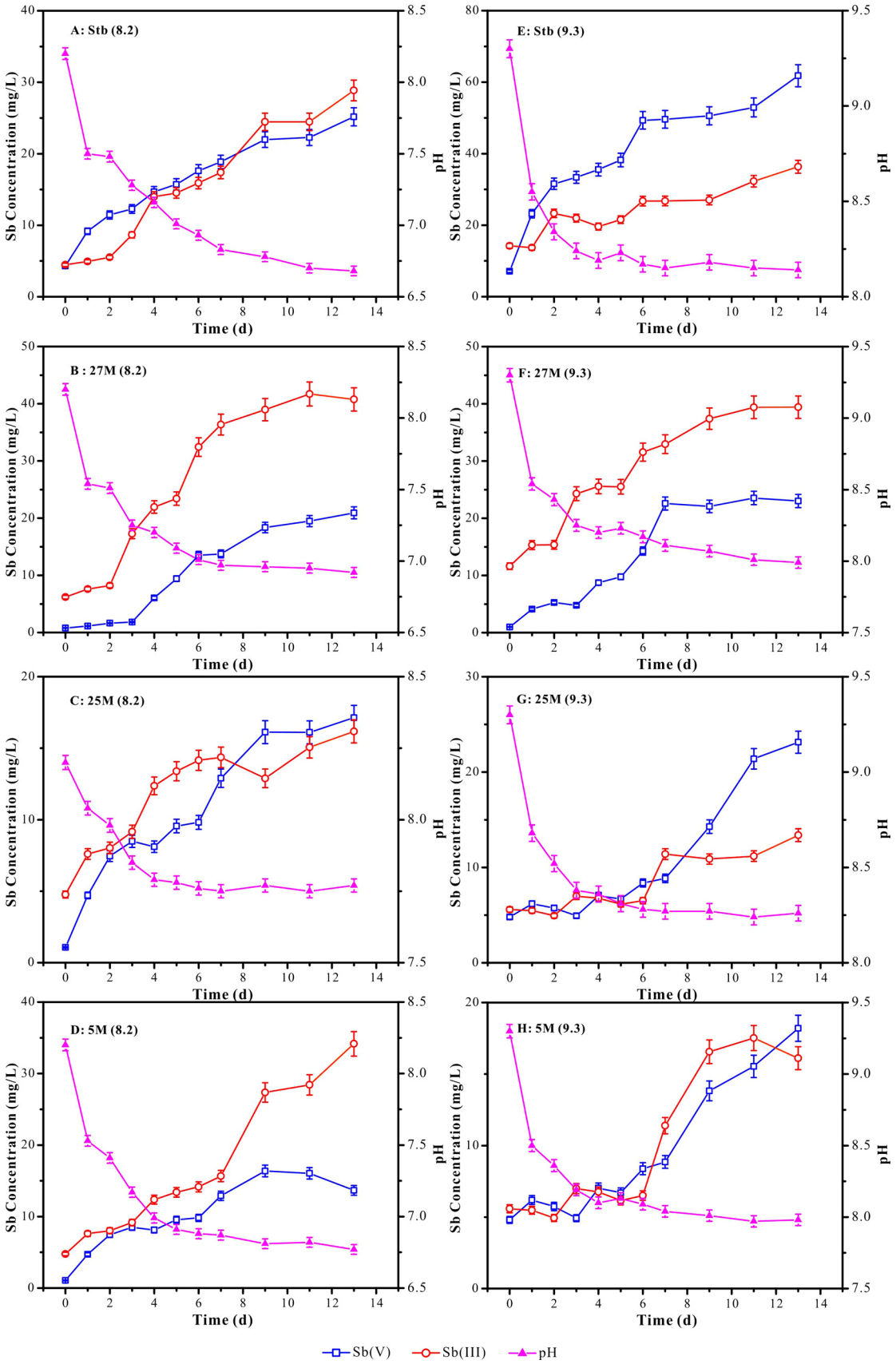

Fig. 5. Variation in pH and concentrations of dissolved Sb(III) and Sb(V) in abiotic systems with different initial pH (A–D, pH 8.2; E–H, pH 9.3). Sample designations are the same with those in Fig. 4. Error bars indicate the standard deviation (n = 2).

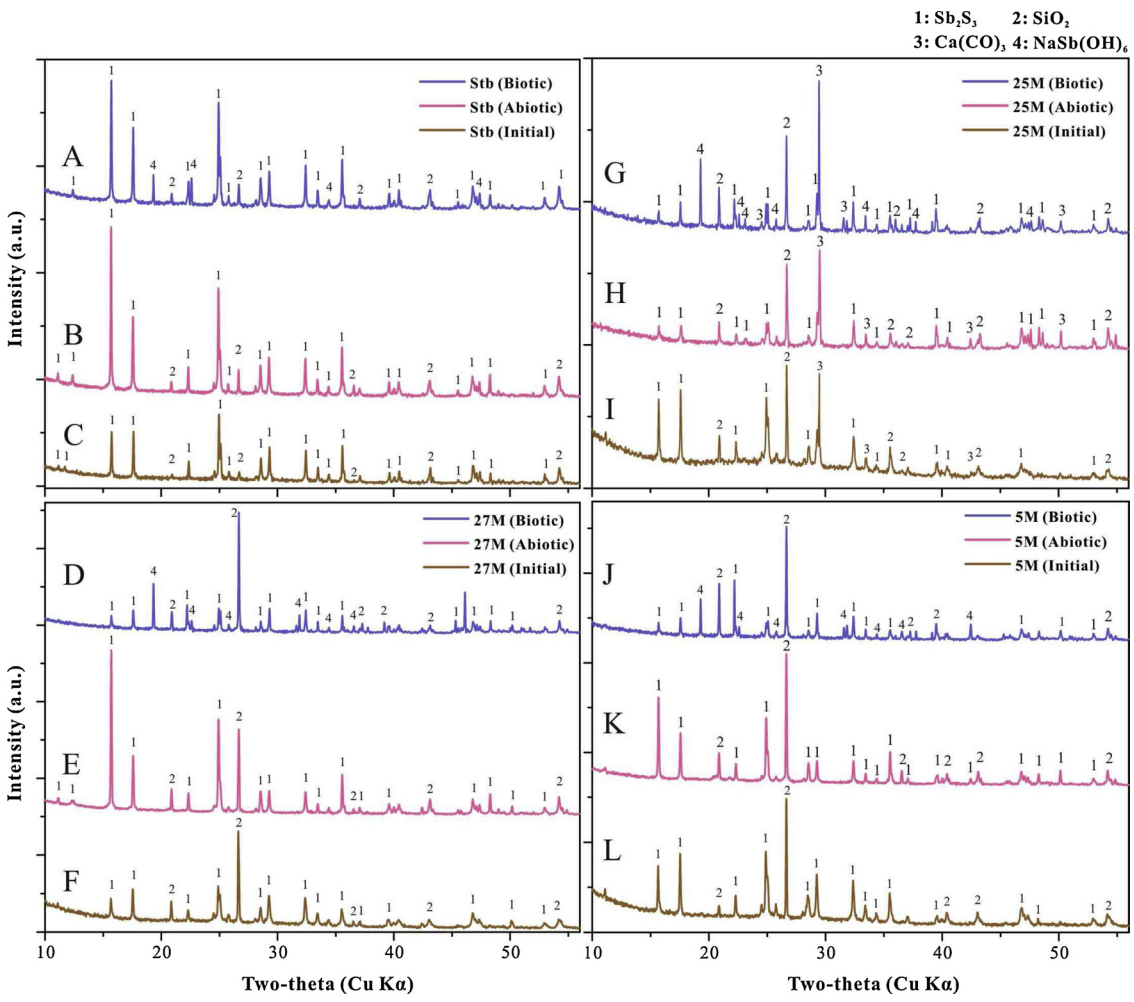

Fig. 6. X-ray diffraction patterns of untreated samples (C, I, F and L), and after 13 days of contact with XT0.6 culture media (A, G, D and J) and the corresponding abiotic controls (B, E, H and K). 1: Stibnite (Sb_2S_3), 2: Quartz (SiO_2), 3: Calcite [$Ca(CO_3)$], 4: Mopungite[$NaSb(OH)_6$].

stibnite contents of the corresponding abiotic samples after 13 days of contact with sterile CDM solution were decreased by 15 %, 16 %, 10 %, and 6.5 % respectively (Table 1).

A secondary Sb(V)-bearing phase mopungite[$NaSb(OH)_6$] was detected in all biotic samples (Fig. 6) and accounted for 8.2 %, 9.8 %, 10.0 % and 10.2 % of the mineralogical content of the standard stibnite, 25 M, 27 M and 5 M samples, respectively (Table 1). The decrease of soluble Sb(V) over time in bacterial cultures is attributed to the formation of mopungite (Fig. 4). In contrast, mopungite was not detected in the abiotic experiments (Fig. S5) despite the higher concentration of total Sb was in the standard stibnite series at initial pH of 9.3 (88 mg/L or 723 µM, Fig. 5E, Table S3) than that in its biotic counterpart (68 mg/L or 559 µM, Fig. 4A). To be noted, the final concentration of Sb(V) in abiotic experiments varied from 0 to 507 µM (Table S3), which are lower than those in the their biotic counterpart systems and may result in the absence of mopungite.

SEM and EDS analyses provided evidence for bacterial attachment on the mineral surfaces as well as morphological changes of mineral particles under abiotic and biotic conditions (Fig. 7). Roughness of Sb-mineral surfaces increased in all biotic samples (Fig. 7B, E, H and K), in striking contrast with the smooth surfaces in the abiotic samples after 13 days' incubation (Fig. 7A, D, G and J). The EDS analyses showed that Sb, S, Si, Na, and Ca were the main components in the abiotic and biotic samples. The dominance of stibnite mineral accounts for the strong peaks of Sb and S in EDS spectrum (Fig. 7C, F, I, and L). The detection of Na peaks in the solid samples from bacterial cultures supports the incorporation of Na in the solid phase, consistent with the detection of mopungite via XRD analysis. Our results provide the evidence that microorganisms can directly play an important role in biogeochemical cycling of antimony through the dissolution and oxidation of Sb-sulfide and the formation of secondary Sb(V)-bearing minerals.

To be noted, an increase in the dissolved Sb concentration was observed with the decrease of stibnite content in rock samples in the biotic systems (Fig. 4, Table 1), indicating the impact of Sb-bearing sulfide content on the dissolution of Sb. Our observation is also consistent with previous report about that the extent of Sb dissolution is negatively correlated with content of Sb in the mineral phase (Hu et al., 2016a). These results infer that at mining areas much attention should be paid to the disposal and management of solid materials such as waste rocks, mining tailings, and smelters with relatively low level of Sb-bearing minerals. The progressive dissolution of Sb(III) from the minerals followed by microbial complete oxidation to Sb(V) decreases the toxicity of Sb(III) to microorganisms and resulted in the accumulation of Sb(V) in the solution. In addition, the replacement of Sb(III)-bearing sulfide, stibnite, with Sb(V)-bearing mopungite which also scavenge part of the dissolved Sb(V) (Multani et al., 2016; Selim, 2012).

3.5. Mechanism of microbial oxidation of Sb-minerals in natural environments

We proposed a two-step model concerning the interaction between Sb-bearing materials and microorganisms in natural environments. As we discussed above about the batch cultures in the lab, bacteria may dissolve Sb(III) in sulfide minerals via increasing pH and subsequently

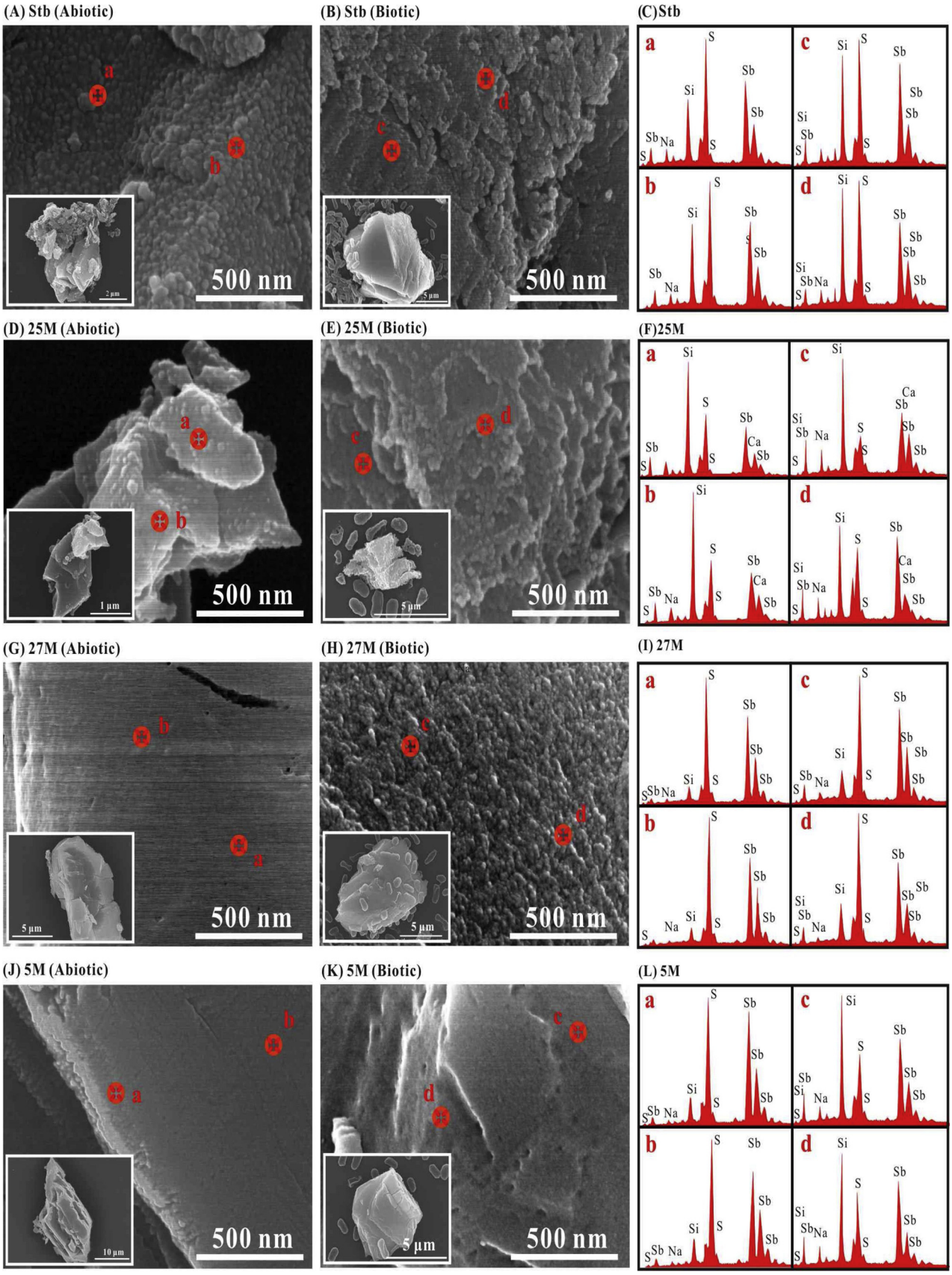

Fig. 7. SEM images of solid phases at the end of experiments (13 days) in the abiotic (A, D, G, J) and biotic (B, E, H, K) treatments. EDS spectra of the solid phases in abiotic (spot a,b) and biotic (spot c,d) treatments are also shown in parallel to the SEM images (C, F, I, L).

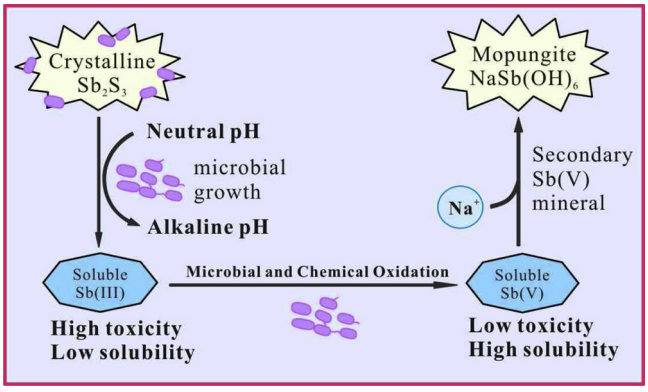

Fig. 8. Schematic representation of the proposed mechanism for Sb(III) dissolution from minerals, the subsequent oxidation to Sb(V), and the formation of Sb(V)-bearing secondary mineral mediated by microorganisms.

oxidize Sb(III) to Sb(V) completely, which result in the formation of Sb (V)-bearing precipitates as secondary minerals (Fig. 8).

At mining sites, Sb-sulfide minerals, low-grade waste ore materials, and tailings provide an attaching substratum for aerobic microorganisms when they expose to the air with mining activities. With bacterial growth the pH around the microbes will increase and lead to the dissolution and subsequently complete oxidation of Sb(III) dissolved (Fig. 8). The accumulation of Sb(V) overtime will result in the formation of mopungite in the presence of available Na^+, which is actually abundant in aquatic environments (Wen et al., 2016), up to 199 mg/L in groundwater at XKS (Nyirenda et al., 2015).

This mechanism greatly enhances our understanding about microbial involvement in the mobilization, oxidation and transformation of Sb(III) in antimony sulfides which are the main Sb-bearing ore minerals at XKS and other mining areas. These ore minerals are often exposed to air with mining activities and become a high-risk pollution source to the surrounding environments. Our results also provide valuable knowledge on the management of mining tailings and waste via inhibition of microbial mobilization of Sb in minerals or formation of secondary Sb-bearing minerals to re-stabilize Sb released.

4. Conclusion

Paraccocus versutus XT0.6 isolated from XKS can oxidize dissolved Sb(III) aerobically and anaerobically. XT0.6 interacts with Sb(III)-bearing minerals/rocks through the dissolution of Sb(III) from Sb-sulfide followed by microbial oxidation, and the formation of secondary Sb (V)-bearing minerals. The dissolution and oxidation alter the toxicity and mobility of Sb, whereas the formation of secondary minerals stabilize part Sb(V) into minerals. All these processes are of significance to understand biogeochemistry of antimony at mining area. In combination with the abiotic results we concluded that both the chemical and microbial factors contribute to the high concentration of Sb(V) in groundwater at XKS. However, microbes can also decrease the Sb(V) concentration to some extent via the formation of secondary Sb(V)-bearing minerals under natural environment, which offer new ideas about Sb(V) bioremediation.

Acknowledgment

This research was supported by the National Science Foundation of China (41877320) and the Fundamental Research Funds for the Central Universities, China University of Geosciences (Wuhan) (CUGCJ1703, CUGQY1922). We thank Wang Nian for help with the construction of the phylogenetic tree based on the whole genome sequencing.

Appendix A. Supplementary data

Supplementary material related to this article can be found, in the online version, at doi:https://doi.org/10.1016/j.jhazmat.2019.121561.

References

Abin, C.A., Hollibaugh, J.T., 2014. Dissimilatory antimonate reduction and production of antimony trioxide microcrystals by anovel microorganism. Environ. Sci. Technol. 48, 681–688.
Asta, M.P., Kirk Nordstrom, D., Blaine McCleskey, R., 2012. Simultaneous oxidation of arsenic and antimony at low and circumneutral pH, with and without microbial catalysis. Appl. Geochem. 27, 281–291.
Biver, M., Shotyk, W., 2012a. Stibnite (Sb_2S_3) oxidative dissolution kinetics from pH 1 to 11. Geochim. Cosmochim. Acta. 79, 127–139.
Biver, M., Shotyk, W., 2012b. Experimental study of the kinetics of ligand-promoted dissolution of stibnite (Sb_2S_3). Chem. Geo. 294–295, 165–172.
Buschmann, J., Sigg, L., 2004. Antimony(III) binding to humic substances: influence of pH and type of humic acid. Environ. sci. Technol. 38, 4535–4541.
Cornelis, R., Caruso, J., Crews, H., Heumann, K.G., 2005. In: Cornelis, R. (Ed.), Handbook of Elemental Speciation 2 Vols: Species in the Environment, Food, Medicine and Occupational Health. Wiley, Chichester pp. 768.
Das, S., Jean, J.S., Chou, M.L., Rathod, J., Liu, C.C., 2016. Arsenite-oxidizing bacteria exhibiting plant growth promoting traits isolated from the rhizosphere of oryza sativa L.: Implications for mitigation of arsenic contamination in paddies. J. Hazard. Mater. 302, 10–18.
Filella, M., Belzile, N., Chen, Y.-W., 2002. Antimony in the environment: a review focused on natural waters: I. Occurrence. Earth-Sci. Rev. 57, 125–176.
Filella, M., Belzile, N., Chen, Y.W., 2003. Antimony in the environment: a review focused on natural waters. Part 2. Relevant solution chemistry. Earth-Sci. Rev. 59, 265–285.
He, M., 2007a. Distribution and phytoavailability of antimony at an antimony mining and smelting area, Hunan, China. Environ. Geochem. Health. 29, 209–219.
He, M., 2007b. Distribution and phytoavailability of antimony at an antimony mining and smelting area, Hunan, China. Environ. Geochem. Health. 29, 209–219.
He, M., Wang, X., Wu, F., Fu, Z., 2012. Antimony pollution in China. Sci. Tot. Environ. 421–422, 41–50.
He, M., Wang, N., Long, X., Zhang, C., Ma, C., Zhong, Q., Wang, A., Wang, Y., Pervaiz, A., Shan, J., 2018. Antimony speciation in the environment: recent advances in understanding the biogeochemical processes and ecological effects. J. Environ. Sci. 75, 14–39.
Herath, I., Vithanage, M., Bundschuh, J., 2017. Antimony as a global dilemma: geochemistry, mobility, fate and transport. Environ. Pollut. 223, 545–559.
Hu, X., He, M., 2017. Organic ligand-induced dissolution kinetics of antimony trioxide. J. Environ Sci. 56, 87–94.
Hu, X., Kong, L., He, M., 2014. Kinetics and mechanism of photopromoted oxidative dissolution of antimony trioxide. Environ. Sci. Technol. 48, 14266–14272.
Hu, X., He, M., Li, S., 2015a. Antimony leaching release from brake pads: effect of pH, temperature and organic acids. J. Environ Sci. 29, 11–17.
Hu, X., He, M., Kong, L., 2015b. Photopromoted oxidative dissolution of stibnite. Appl. Geochem. 61, 53–61.
Hu, X., Guo, X., He, M., Li, S., 2016a. pH-dependent release characteristics of antimony and arsenic from typical antimony-bearing ores. J. Environ Sci. 44, 171–179.
Hu, X., Guo, X., He, M., Li, S., 2016b. pH-dependent release characteristics of antimony and arsenic from typical antimony-bearing ores. J. Environ. Sci. 44, 171–179.
Hu, X., He, M., Li, S., Guo, X., 2017. The leaching characteristics and changes in the leached layer of antimony-bearing ores from China. J. Geochem Explor. 176, 76–84.
Jinming, L., Xubiao, L., John, C., Jiuhui, Q., Yaohui, B., Yue, P., Junhua, L., 2015. Removal of antimonite Sb(III) and antimonate Sb(v) from aqueous solution using carbon nanofibers that are decorated with zirconium oxide (ZrO2). Environ. Sci. Technol. 49, 11115–11124.
Kaksonen, A.H., Franzmann, P.D., Puhakka, J.A., 2003. Performance and ethanol oxidation kinetics of a sulfate-reducing fluidized-bed reactor treating acidic metal-containing wastewater. Biodegradation. 14, 207–217.
Khan, U.A., Kujala, K., Nieminen, S.P., Räisänen, M.L., Ronkanen, A.-K., 2019. Arsenic, antimony, and nickel leaching from northern peatlands treating mining influenced water in cold climate. Sci. Tot. Environ. 657, 1161–1172.
Kong, L.-T., Zhang, M., Liu, X., Ma, F.-Y., Wei, B., Wumaier, K., et al., 2019. Green and rapid synthesis of iron molybdate catalyst by mechanochemistry and their catalytic performance for the oxidation of methanol to formaldehyde. Chem. Eng. J. 364, 390–400.
Kulp, T.R., Miller, L.G., Braiotta, F., Webb, S.M., Kocar, B.D., Blum, J.S., Oremland, R.S., 2015. Microbiological reduction of Sb(v) in anoxic freshwater sediments. Environ. Sci. Technol. 48, 218–226.
Lehr, C.R., Kashyap, D.R., Mcdermott, T.R., 2007. New insights into microbial oxidation of antimony and arsenic. Appl. Environ. Microbiol. 73, 2386.
Leuz, A.-K., Johnson, C.A., 2005. Oxidation of Sb(III) to Sb(v) by O_2 and H_2O_2 in aqueous solutions. Geochim. Cosmochim. Acta. 69, 1165–1172.
Leuz, A.-K., Mönch, H., Johnson, C.A., 2006. Sorption of Sb(III) and Sb(v) to goethite: influence on Sb(III) oxidation and mobilization. Environ. sci. Technol. 40, 7277–7282.
Li, J., Wang, Q., Zhang, S., Qin, D., Wang, G., 2013. Phylogenetic and genome analyses of antimony-oxidizing bacteria isolated from antimony mined soil. Int. Biodeterior. Biodegrad. 76, 76–80.
Li, J., Wang, Q., Li, M., Yang, B., Shi, M., Guo, W., McDermott, T.R., Rensing, C., Wang,

G., 2015. Proteomics and genetics for identification of a bacterial antimonite oxidase in agrobacterium tumefaciens. Environ. Sci. Technol. 49, 5980–5989.
Li, J., Wang, Q., Oremland, R.S., Kulp, T.R., Rensing, C., Wang, G., 2016a. Microbial antimony biogeochemistry: enzymes, regulation, and related metabolic pathways. Appl. Environ. Microbiol. 82, 5482–5495.
Li, Y., Liu, Z., Li, Q., Liu, F., Liu, Z., 2016b. Alkaline oxidative pressure leaching of arsenic and antimony bearing dusts. Hydrometallurgy. 166, 41–47.
Li, J., Yang, B., Shi, M., Yuan, K., Guo, W., Wang, Q., Wang, G., 2017. Abiotic and biotic factors responsible for antimonite oxidation in *Agrobacterium tumefaciens* GW4. Sci. Rep. 7, 43225.
Li, J., Yu, H., Wu, X., Shen, L., Liu, Y., Qiu, G., Zeng, W., Yu, R., 2018. Novel hyper antimony-oxidizing bacteria isolated from contaminated mine soils in China. Geomicrobiol J. 35, 713–720.
Liu, F., Le, X.C., McKnight-Whitford, A., Xia, Y., Wu, F., Elswick, E., Johnson, C.C., Zhu, C., 2010. Antimony speciation and contamination of waters in the Xikuangshan antimony mining and smelting area, China. Environ. Geochem. Health. 32, 401–413.
Liu, D., Dong, H., Bishop, M.E., Zhang, J., Wang, H., Xie, S., Wang, S., Huang, L., Eberl, D.D., 2012. Microbial reduction of structural iron in interstratified illite-smectite minerals by a sulfate-reducing bacterium. Geobiology. 10, 150–162.
Lu, X., Zhang, Y., Liu, C., Wu, M., Wang, H., 2018. Characterization of the antimonite- and arsenite-oxidizing bacterium *Bosea* sp. AS-1 and its potential application in arsenic removal. J. Hazard. Mater. 359, 527–534.
Multani, R.S., Feldmann, T., Demopoulos, G.P., 2016. Antimony in the metallurgical industry: a review of its chemistry and environmental stabilization options. Hydrometallurgy. 164, 141–153.
Nepple, B.B., Flynn, I., Bachofen, R., 1999. Morphological changes in phototrophic bacteria induced by metalloid oxyanions. Microbiol. Res. 154, 191–198.
Nguyen, V.K., Lee, J.-U., 2015. Antimony-oxidizing bacteria isolated from antimony-contaminated sediment – a phylogenetic study. Geomicrobiol J. 32, 50–58.
Nguyen, V.K., Tran, T., Han, H.-J., Lee, S.-H., Lee, J.-U., 2015. Possibility of bacterial leaching of antimony, chromium, copper, manganese, nickel, and zinc from contaminated sediment. J. Geochem. Explor. 156, 153–161.
Nguyen, V.K., Choi, W., Yu, J., Lee, T., 2017. Microbial oxidation of antimonite and arsenite by bacteria isolated from antimony-contaminated soils. Int. J Hydrogen Energ. 42, 27832–27842.
Nyirenda, T.M., Zhou, J., Xie, L., Pan, X., Li, Y., 2015. Determination of carbonate minerals responsible for alkaline mine drainage at Xikuangshan antimony mine, China: using thermodynamic themical equilibrium model. J. Earth Sci. 26, 755–762.
Paul, D., Kazy, S.K., Banerjee, T.D., Gupta, A.K., Pal, T., Sar, P., 2015. Arsenic biotransformation and release by bacteria indigenous to arsenic contaminated groundwater. Bioresour. Technol. 188, 14–23.
Salmassi, T.M., Venkateswaren, K., Satomi, M., Newman, D.K., Hering, J.G., 2002. Oxidation of arsenite by *Agrobacterium albertimagni*, AOL15, sp. nov., Isolated from hot creek, California. Geomicrobiol J. 19, 53–66.
Selim, H.M., 2012. In: Selim, H.M. (Ed.), Competitive Sorption and Transport of Heavy Metals in Soils and Geological media. CRC Press, Florida, USA, pp. 119–145.
Shi, Z., Cao, Z., Qin, D., Zhu, W., Wang, Q., Li, M., Wang, G., 2013. Correlation models between environmental factors and bacterial resistance to antimony and copper. Plos One. 8, e78533.
Sun, W., Xiao, E., Dong, Y., Tang, S., Krumins, V., Ning, Z., Sun, M., Zhao, Y., Wu, S., Xiao, T., 2016. Profiling microbial community in a watershed heavily contaminated by an active antimony (Sb) mine in Southwest China. Sci. Tot. Environ. 550, 297–308.
Terry, L.R., Kulp, T.R., Wiatrowski, H., Miller, L.G., Oremland, R.S., 2015. Microbiological oxidation of antimony(III) with oxygen or nitrate by bacteria isolated from contaminated mine sediments. Appl. Environ. Microbiol. 81, 8478–8488.
Wang, Q., He, M., Wang, Y., 2011. Influence of combined pollution of antimony and arsenic on culturable soil microbial populations and enzyme activities. Ecotoxicology. 20, 9–19.
Wang, N., Zhang, S., He, M., 2016. Bacterial community profile of contaminated soils in a typical antimony mining site. Env Sci. Pollut Res. 25, 1–12.
Weeger, W., Lièvremont, D., Perret, M., Lagarde, F., Hubert, J.-C., Leroy, M., Lett, M.-C., 1999. Oxidation of arsenite to arsenate by a bacterium isolated from an aquatic environment. Biometals. 12, 141–149.
Wen, B., Zhou, J., Zhou, A., Liu, C., Xie, L., 2016. Sources, migration and transformation of antimony contamination in the water environment of Xikuangshan, China: evidence from geochemical and stable isotope (S, Sr) signatures. Sci. Tot. Environ. 569–570, 114–122.
WHO, 1996. Guidelines for drinking-water quality. Vol. 2. Health Criteria and Other Supporting Information, 2nd ed. World Health Organization 937.
Wilson, S.C., Lockwood, P.V., Ashley, P.M., Tighe, M., 2010. The chemistry and behaviour of antimony in the soil environment with comparisons to arsenic: a critical review. Environ. Pollut. 158, 1169–1181.
Xiao, E., Krumins, V., Tang, S., Xiao, T., Ning, Z., Lan, X., Sun, W., 2016. Correlating microbial community profiles with geochemical conditions in a watershed heavily contaminated by an antimony tailing pond. Environ. Pollut. 215, 141–153.
Zhang, S.-Y., Williams, P.N., Luo, J., Zhu, Y.-G., 2016. Microbial mediated arsenic biotransformation in wetlands. Front. Environ. Sci. Eng. 11, 1.
Zhang, S.Y., Su, J.Q., Sun, G.X., Yang, Y., Zhao, Y., Ding, J., Chen, Y.S., Shen, Y., Zhu, G., Rensing, C., 2017. Land scale biogeography of arsenic biotransformation genes in estuarine wetland. Environ. Microbiol. 19.
Zhou, W., Yan, W., Li, N., Li, Y., Dai, Y., Zhang, Z., Ma, S., 2019. Fabrication of mullite-corundum foamed ceramics for thermal insulation and effect of micro-pore-foaming agent on their properties. J. Alloys. Compds. 785, 1030–1037.